

The origin of an efficiency improving “light soaking” effect in SnO₂ based solid-state dye-sensitized solar cells

Priti Tiwana, Pablo Docampo, Michael B. Johnston, Laura M. Herz and Henry J. Snaith*

Received 23rd May 2012, Accepted 28th August 2012

DOI: 10.1039/c2ee22320a

We observe a strong “light-soaking” effect in SnO₂ based solid-state dye-sensitized solar cells (SDSCs). Both with and without the presence of UV light, the device’s short-circuit photocurrent and efficiency increase significantly over 20–30 minutes, until steady-state is achieved. We demonstrate that this is not due to improved charge collection and investigate the charge generation dynamics employing optical-pump terahertz-probe spectroscopy. We observe a monotonic speeding-up of the generation of free-electrons in the SnO₂ conduction band as a function of the light-soaking time. This improved charge generation can be explained by a positive shift in the conduction band edge or, alternatively, an increase in the density of states (DoS) at the energy at which photoinduced electron transfer occurs. To verify this hypothesis, we perform capacitance and charge extraction measurements which indicate a shift in the surface potential of SnO₂ of up to 70 mV with light soaking. The increased availability of states into which electrons can be transferred justifies the increase in both the charge injection rate and ensuing photocurrent. The cause for the shift in surface potential is not clear, but we postulate that it is due to the photoinduced charging of the SnO₂ inducing a rearrangement of charged species or loss of surface oxygen at the dye-sensitized heterojunction. Understanding temporally evolving processes in DSCs is of critical importance for enabling this technology to operate optimally over a prolonged period of time. This work specifically highlights important changes that can occur at the dye-sensitized heterojunction, even without direct light absorption in the metal oxide.

Introduction

TiO₂ is the most commonly employed oxide in dye-sensitized solar cells (DSCs) and represents the highest efficiency electrode employed to date. However, in many respects the electronic properties of SnO₂ should be superior and as such it has raised

interest in the DSC community.^{1–3} The main drivers for employing SnO₂ are its high band-gap resulting in low photocatalytic activity, which should lead to increased device stability (though not proven to date) and that the bulk mobility of SnO₂ is almost 2 orders of magnitude higher than that of TiO₂.^{4,5} Hence, there is potential for fabricating mesoporous SnO₂ films with high mobility which result in significantly higher charge collection efficiency under working conditions, and reduced series resistance losses which should result in improved fill factors and

University of Oxford, Department of Physics, Clarendon Laboratory, Parks Road, Oxford OX1 3PU, UK. E-mail: h.snaith1@physics.ox.ac.uk

Broader context

Recently, significant effort has been invested in designing high performance solid-state dye-sensitized solar cells (SDSCs) which can work consistently over a few years. Theoretically, higher device efficiency is possible if the more popularly used TiO₂ electrode is replaced with SnO₂. While this goal has not yet been achieved, various researchers have reported different methods for optimising the SnO₂-based device performance. A well-established observation in TiO₂-based liquid electrolyte DSCs is that the device performance improves significantly after exposure to UV light for time-periods ranging from minutes to months. In this paper, we report, for the first time, an analogous dramatic light-soaking effect in solid-state DSCs fabricated with SnO₂. While TiO₂ devices work better in the presence of UV illumination, SnO₂ devices show improvement even under red light illumination. A clear understanding of such temporally evolving processes in DSCs is crucial if we want to design solar cells which exhibit high performance immediately after installation, and which can operate optimally over a prolonged period of time. In this work, we have employed a range of device-based and spectroscopic techniques with time-scales ranging from femtoseconds to milliseconds in order to understand the underlying mechanism for the light-soaking effect.

efficiency.^{1,2,6} Additionally, the SnO₂ conduction band (CB) edge is between 350 and 500 mV more positive than that of TiO₂,⁶ which implies that SnO₂ should be more suitable for use with very narrow band-gap sensitizers, opening prospects for tandem DSCs.

Despite all these potential advantages of SnO₂, various research groups have shown that the performance of “bare” SnO₂-based solar cells, where there is no surface treatment of the SnO₂ mesoporous film, is relatively low and is limited by both poor short-circuit current (J_{SC}) and open-circuit voltage (V_{OC}) due to severe recombination losses. A popular solution to the problem is to apply a conformal coating of a high band-gap material such as MgO, Al₂O₃, ZrO₂ or TiO₂ upon the internal surface of the SnO₂ nanoparticles.^{1-3,7-9} This treatment results in a dramatic improvement in device efficiency by primarily enhancing the V_{OC} , and also the J_{SC} to some extent, both in liquid-electrolyte^{2,3,7-9} and solid-state DSCs.^{1,10} For solid-state DSCs (SDSCs) there is almost a 3–5 fold reduction in the recombination rate when the SnO₂ nanoparticles have a sub-nm shell of MgO around them, and further still with a shell of TiO₂.¹ However, for SDSCs it is also important to prevent direct contact of the top metallic electrode with the mesoporous SnO₂, since this can result in a shunting path which impacts upon open-circuit voltage and photocurrent.¹¹

Here, for SnO₂-based SDSCs employing spiro-OMeTAD as the hole-transporter, we have observed an unexpected light soaking phenomenon where a significant improvement in short-circuit photocurrent occurs as a function of the exposure time to sunlight (simulated by a solar simulator or LEDs). Generally the devices are “light-soaked” for up to 20 minutes before the photocurrent stabilizes. Similar light soaking phenomena have been observed many times previously for TiO₂ based solar cells, but this effect is usually interpreted as being due to direct absorption of UV light in the TiO₂ layer.¹²⁻¹⁵ Here the primary objective of employing SnO₂ is to circumvent these types of phenomena. However we still observe a strong light soaking effect, even when light is only absorbed in the dye (not oxide nor hole-transporter). To understand the mechanism, we have employed terahertz pump-probe spectroscopy, which determines the rate and magnitude of photogenerated electrons in the SnO₂. We observe an increase in both the electron injection rate and the overall photoconductivity signal with exposure time, which is the first time that temporally evolving injection kinetics have been observed in DSCs. This direct measurement indicates that light-soaking enhances photoinduced electron transfer, but notably, without the requirement for any direct light absorption in the metal oxide. The light soaking phenomenon appears to be, simply, a result of the charging of the solar cell.

Results and discussion

The devices studied here are fabricated from mesoporous SnO₂ coated with a thin shell of MgO and sensitized with a visible absorbing indolene dye termed D102.^{16,17} We have previously demonstrated that this specific system can generate charge very efficiently, with an estimated absorbed photon-to-electron conversion efficiency (APCE) of close to unity.¹ However, to obtain optimum performance of these devices, they are required to be exposed to light, or “light soaked”, for up to 20 minutes.

Typically, this is done under open-circuit conditions in our experimental set-up. This is illustrated in Fig. 1a, where we show typical current–voltage curves measured after exposing MgO-treated SnO₂-based SDSC devices to simulated sunlight over a period of 18 minutes. A steady improvement in both J_{SC} and device efficiency is observed over a period of about 20–30 minutes till steady-state is achieved, as shown in Fig. 1b. The fill-factor (FF) improves marginally while a slight decrease in V_{OC} is observed over this measurement time, as shown in Fig. 1c. A light soaking effect has been previously observed for TiO₂ based liquid electrolyte DSCs,^{14,15,18,19} with the enhancement occurring over time periods ranging from hours to days to even months. However such phenomena are not usually observed in solid-state cells, and certainly not to the extent observed here, where the photocurrent more than doubles over the measurement time. For electrolyte based TiO₂ DSCs, it has been interpreted by considering the influence of ultraviolet light upon the TiO₂ surface states.¹²⁻¹⁵ UV exposure of TiO₂ can result in increased oxygen vacancy density which results in a relative positive shift in the surface potential. Dye-sensitizers which were previously poor at

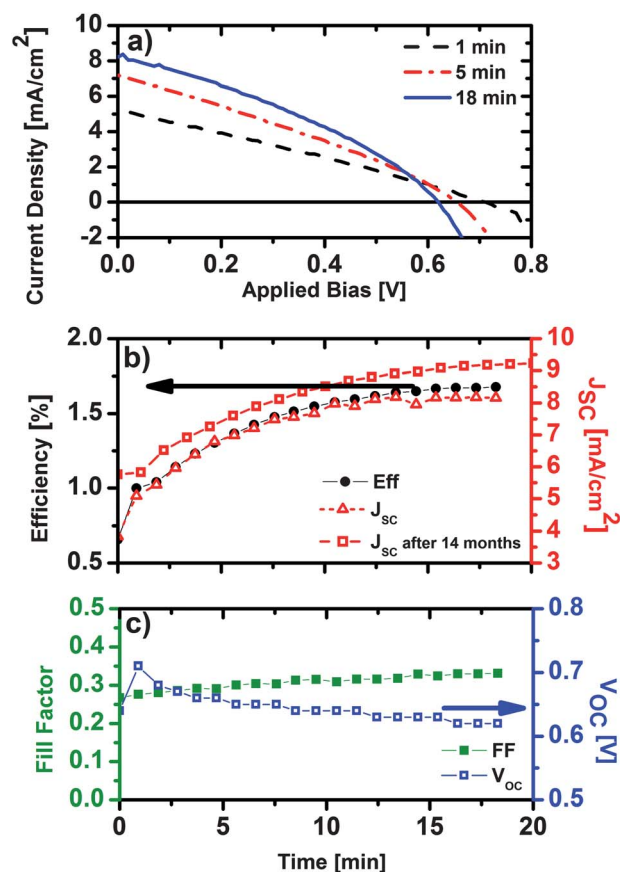


Fig. 1 Typical current–voltage (JV) measurements for solid-state DSCs incorporating MgO-treated SnO₂ sensitized with D102. (a) JV curves measured at different times after exposure to simulated AM1.5G sunlight at 100 mW cm⁻² equivalent intensity. (b) Device efficiency and J_{SC} show a steady increase over 20–30 minutes until steady state is achieved. The short-circuit current evolution was re-measured after 14 months on a similar device, measured under a white LED array where no UV light was present, as shown by red open squares. (c) Change in fill factor (FF) and V_{OC} as a function of time under simulated AM1.5G light soaking at 100 mW cm⁻² irradiance.

injecting charge into the TiO₂ then become capable of undergoing efficient photoinduced electron transfer and the photocurrent and efficiency increase.¹² Here, we observe this phenomenon in SnO₂ based cells, where the band gap of SnO₂ is approximately 3.8 eV, compared with 3.2 eV for TiO₂.⁶ To test whether UV absorption in the SnO₂ is at the root of this phenomenon, we measured some devices under exposure to white light generated from an array of LEDs (LXHL-NWE8) where there is no light emitted with a wavelength lower than 400 nm (3.1 eV). In Fig. 1b we also show the evolution of a device J_{SC} under such illumination (red open squares), and once again the same trend with increasing photocurrent over 20 minutes is observed. The devices return to their pre-illuminated state after being left in the dark for about 30 minutes, illustrating that the process occurring is reversible. Remarkably, the device shown in Fig. 1b was analysed 14 months after fabrication (stored in air in the dark without encapsulation) and exactly the same “kinetics” are observed, indeed even 2 years after fabrication the performance remains the same. To further conclude that UV light is not required, the same trends in increasing photocurrent are also observed when the device is illuminated with red LEDs (not shown). JV measurements carried out on SnO₂ SDSCs without MgO treatment show poorer efficiency and J_{SC} values,^{1,10} and are therefore not discussed here, though the comparison will be the subject of a separate publication.¹⁰

Since high-energy (UV) photons are clearly not a prerequisite for the observed light-soaking effects, it appears that photoinduced charge generated in the device is responsible, and not necessarily a chemical change to the oxide surface under direct light absorption. Before we try and deduce the mechanism however, we need to determine if this improvement in photocurrent is due to enhanced charge collection (*i.e.* fewer losses due to recombination of free electrons and holes) or enhanced charge generation. In order to probe the charge collection, we carried out a series of small perturbation transient photovoltage and photocurrent decay measurements on the SnO₂-MgO/D102 SDSCs under short-circuit conditions. The technique is outlined in the Experimental details section. The white light bias was maintained at an equivalent of 100 mW cm⁻² irradiance (as set

with a KG5 filtered calibrated Si reference diode) for comparison with the results obtained under simulated sunlight. Typical trends for the transport and recombination rates are shown in Fig. 2. We find that the electron transport rate k_{trans} increases as a direct result of exposure to light. Surprisingly however, we also find that the recombination rate k_{rec} increases, but marginally faster than the transport, negating any potential improvements from faster charge collection. This is in contrast to the longer term light soaking study performed by Listorti *et al.* on TiO₂ based electrolyte cells who found a notable reduction in the recombination rate as a function of light soaking.¹⁸ An estimate of the charge collection efficiency (η_{coll}) can be obtained from these measurements by simply balancing the rates for charge collection and recombination, as below:

$$\eta_{coll} = \frac{k_{trans}}{k_{trans} + k_{rec}} \quad (1)$$

Contrary to expectations, therefore, in Fig. 2 we show that η_{coll} (red stars) decreases as a result of light-soaking, even though J_{SC} (red diamonds) measured simultaneously during the same experiment is seen to increase with time. These measurements indicate that improved charge collection is not the cause for the enhanced photocurrent under light soaking.

As an aside, we note that there is a caveat to the transient photocurrent and photovoltage measurements: The maximum photocurrent we could generate under 100 mW cm⁻² AM1.5G sunlight with this sensitizer in solid-state DSCs (2 μ m thick) is around 11 mA cm⁻² if the absorbed photon-to-current collection efficiency (APCE) was unity.¹ We are confident in the calibration of our solar simulator (see the Experimental details section) and hence obtaining up to 9 mA cm⁻² indicates at most a loss of 10 to 20% in charge collection. In contrast the charge collection efficiency here is estimated to drop to around 0.65 after light exposure indicating an inconsistency. It is not the purpose of this work to understand this discrepancy between the steady-state and transient measurements, but it is an issue which ourselves and others are investigating.²⁰⁻²⁹

Assuming the trend observed in the transient measurements to be correct, and that improved charge collection is not the cause for the enhanced photocurrent, we have to consider what other factors could be at play. Photocurrent is a product of the absorbed light, charge generation efficiency and charge collection efficiency. The charge collection appears not to improve and the films do not appear to change considerably in colour, hence charge generation is most likely to influence this improvement in photocurrent under illumination. A recent study on long term light soaking effects in TiO₂ based DSCs by Listorti *et al.* showed a strong correlation between enhanced photoluminescence quenching rates of the dye-sensitizer and enhanced photocurrent. This finding is interpreted to imply that enhanced electron transfer in that system is the mechanism behind the increase in photocurrent.¹⁸ This correlation is surprising, not because of the inferred mechanism, but since the time-correlated single photon counting technique employed has a temporal resolution on the 100 ps timescale, which is much slower than the typical observed electron transfer rate of fs to ps.

In order to directly probe the electron transfer process in this system and to shed more light upon the possible correlation between fs and ns measurement techniques, we have employed

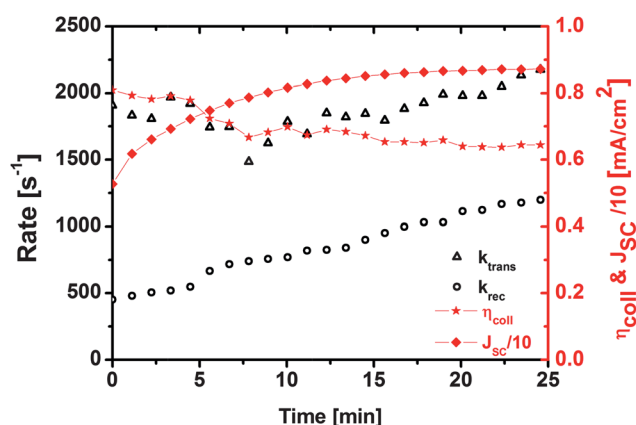


Fig. 2 Transport (black open triangles) and recombination (black open circles) rates as a function of light-soaking time, along with short-circuit current (red diamonds) and estimated charge collection efficiency (red stars), determined by transient photovoltage and photocurrent measurements performed under short-circuit conditions.

optical-pump terahertz-probe (OPTP) spectroscopy on dye-sensitized SnO₂ films. These measurements have been conducted using the ruthenium-based sensitizer termed Z907 (ref. 30 and 31) since the organic dye D102, which operates best in the solar cells, degrades when photoexcited during the OPTP measurements (less photostable). The SnO₂-Z907 films were photoexcited with very short duration pulses (~40 fs) at 550 nm wavelength. The photoexcitation fluence was equivalent to the photon densities absorbed by the cells when exposed to simulated sunlight at 100 mW cm⁻² irradiance. The 550 nm photons are absorbed by the dye and promote it to the excited state, from which photo-induced electron transfer occurs into the SnO₂ CB due to a favorable electronic driving force. These relatively mobile CB electrons interact with the weak terahertz (THz) probe pulse incident on the sample at time τ after the initial excitation pulse. The amount of THz radiation absorbed gives a direct measure of the product of the number and mobility of charge carriers in the photoexcited sample.

Fig. 3a shows the rise in photoconductivity in SnO₂-Z907 samples over the first 15 picoseconds after photoexcitation at 550 nm. As noted earlier, this increase is primarily due to electron

transfer from dye photoexcited states into the SnO₂ CB. The different curves show successive scans, where each scan took about 70 minutes to complete. It is interesting to see that as time progresses, both the charge injection rate and the peak photoconductivity value ($\Delta\sigma$) increase significantly, until “steady-state” is achieved after a few hours of exposure to the light pulse train. The trend can be seen more distinctly in the long-time scans shown in Fig. 3b. The shape of the steady-state curve achieved after 13 hours (red curve in Fig. 3b) is quite different from the previous scans. The final red curves show that once steady state is achieved, there are only two fast electron transfer phases (fs and sub-100 ps), and the slower injection phase (longer than 100 ps) is no longer present. In our previous work comparing TiO₂, SnO₂ and ZnO in both DSCs and OPTP measurements, we have correlated the relative fraction of fast to slow injection phase with charge generation efficiency.⁶ The fast phase is clearly least likely to suffer from competition with other loss mechanisms in the photoexcited dye (*e.g.* natural decay), and therefore these OPTP measurements here are perfectly consistent with the increase in photocurrent observed in the solar cells as a function of illumination time. It should be noted that the absolute electron

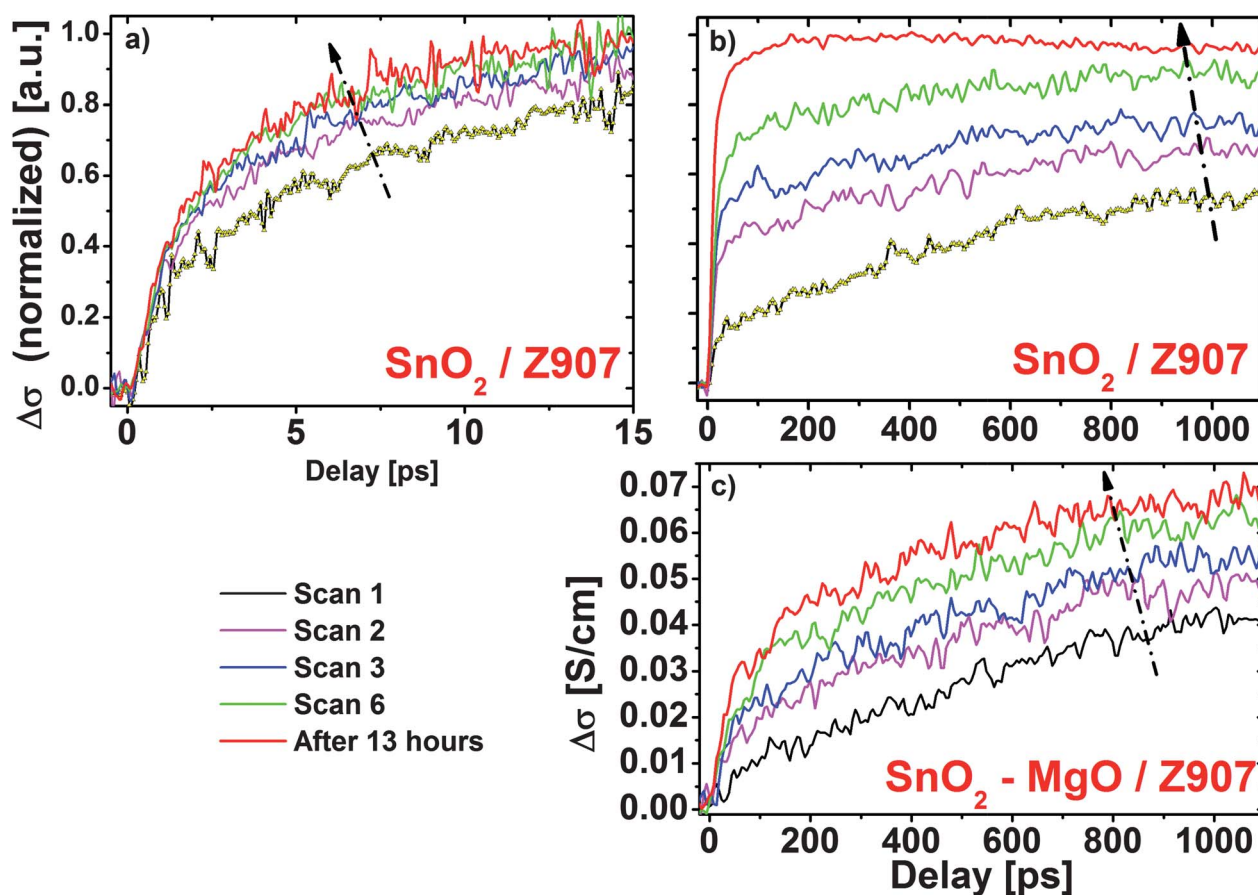


Fig. 3 (a) Early time photoconductivity dynamics in Z907-sensitized SnO₂. Each scan was 71 minutes long and all scans were carried out in succession, without a break; (b) long-time photoconductivity scans, each 38 minutes long. Note (a) and (b) are separate measurements. Curves in (a) and (b) have been normalised so that the peak photoconductivity value (at ~15 ps, red curve in (a), and at ~250 ps, red curve in (b) is 1. (c) Long-time scans measured on SnO₂ with a conformal MgO coating, sensitized with Z907, each 22 minutes long. In all cases, the red curve at the top shows the final “steady-state” trend measured after at least 13 hours of continuous photoexcitation. Photoexcitation was carried out with 550 nm wavelength 40 fs pulses with $\sim 7 \times 10^{14}$ photons cm⁻² fluence on samples kept under vacuum.

injection rate can be different when the dye-sensitized SnO₂ film is embedded in a medium different from air or vacuum, such as in an electrolyte or hole-transporting material.^{32–34}

The above measurements were performed on “bare” SnO₂ sensitized with Z907, but to be more consistent with the solar cells we also performed OPTP spectroscopy on SnO₂ films coated with a thin shell of MgO and sensitized with Z907 dye (SnO₂–MgO/Z907), shown in Fig. 3c. As seen with the bare films, the charge injection rate and photoconductivity are seen to rise steadily with each successive scan. This suggests a similar effect in MgO-treated SnO₂ films, in excellent agreement with the *JV* measurements shown on SnO₂–MgO based SDSCs in Fig. 1. We note that the overall injection rate is slower for the MgO coated dye-sensitized photoanodes, however, this will be discussed in detail in the context of device based results in a subsequent publication.¹⁰

The same trend of light-exposure dependent increase in photoconductivity is observed when photoexcitation is carried out with half the fluence, indicating that the light-soaking effect is a feature of the material combination, and not just an artifact due to high excitation fluences. For this case of photoexcitation at 550 nm at lower energy, the absorbed photon fluence in SnO₂–Z907 is approximately 7.5×10^{16} photons cm⁻² s⁻¹. In comparison, the corresponding absorbed photon fluence in the SnO₂–MgO/D102 devices exposed to AM1.5G light at 100 mW cm⁻² is equivalent to about 7×10^{16} photons cm⁻² s⁻¹ when integrated between 300 and 800 nm (minimum and maximum limits set by the solar spectrum and SnO₂–MgO/D102 absorption respectively). While these figures cannot be directly compared because the OPTP samples are excited with femto-second duration pulses at 500 Hz repetition rate compared to steady-state illumination of the solar cells, this suggests that the exposure is roughly equivalent.

To the best of our knowledge, this is the first time such light soaking effects have been observed, or reported, while performing ultra-fast spectroscopy. To put it in context with the time resolved photoluminescence results of Listorti *et al.*,¹⁸ we would expect to be able to observe some of these initial changes under light soaking employing time-correlated single photon counting (TCSPC) with a 60 ps time resolution. However, the rapid increase in the ps rise component is beyond the time resolution for TCSPC and would hence be missed by that technique. Notably however, in broader context, ultra-fast time resolved measurements typically take a number of hours to align the samples and obtain a measurable signal and are often performed at equivalent CW intensities far above 1 sun illumination. It is not impossible to conceive therefore that most reports of entirely fs electron transfer phenomena are measuring light soaked films where these favorable improvements may have already occurred. Of course this is justifiable to compare with similarly stabilized solar cells.

These early time photoconductivity trends confirm that light soaking of the dye-sensitized SnO₂ film leads to improved charge generation, consistent with the increased photocurrent and device performance. However, the cause for the increased electron transfer rate and efficiency is not directly apparent. To summarize the findings: (1) we have demonstrated that the presence of a UV component is not critical for device improvement, nor spectroscopic observation, eliminating the hypothesis

that direct light absorption in the metal oxide results in the creation of new surface states and a resultant positive shift in the conduction band edge. (2) The process is relatively slow yet reversible. (3) Since it appears in both the “bare” dye-sensitized films and the MgO coated films, it is not an artifact of the surface coating. (4) It is not explicitly a result of lithium TFSI salt migration or redistribution,^{12,19} nor does it result from a change in photodoping of the hole-transporter since it is observed by OPTP spectroscopy in the neat dye-sensitized films. We also note that in the case of red light illumination negligible light is absorbed in the hole-transporter.

It appears evident therefore that the build-up of electronic charge in the SnO₂ is triggering this favorable trend. There are two possible explanations that we can envisage: the first is that the net negative charge of the SnO₂ forces a rearrangement of charged states or species at the surface of the metal oxide, which could cause a shift in surface potential or indeed alter the precise energy distribution of the sub-bandgap states. These species could be protons, partially reduced Sn⁴⁺ states or hydroxide species. The second is related but arises from considering the nature of the bonding between the oxygen and tin ions in the oxide material. With the bonding being predominantly ionic, we could envisage that localized negative charge trapped in surface states could have a very strong influence, weakening the local binding strength between the Sn ions centered on the trap sites and the negatively charged surface oxygen. Hence the increased concentration of localized electrons under illumination could alter to a certain extent the surface oxygen vacancy density. For the more studied oxide, TiO₂, when oxygen vacancies are generated, partially reduced Ti⁴⁺ states are thought to induce sub-bandgap states around ~1 eV below the conduction band.^{35,36} We expect a similar effect in SnO₂. To verify the influence of light-soaking upon the distribution of sub-bandgap states in SnO₂, we have measured the evolution of the DoS with time *via* the transient photovoltage–photocurrent technique for a device illuminated with red light, shown in Fig. 4a. We observe a clear shift of the capacitance (which is proportional to the DoS) towards lower potentials without any significant change to the slope of the curve, consistent with a shift in the surface potential of the SnO₂. It does not entirely rule out however a change in the distribution of sub-bandgap states. In order to discriminate between these two possibilities, we have followed the method of Miettunen *et al.*, where the total extracted charge for a given photocurrent is measured.³⁷ If the trap density increases with respect to the conduction band edge, *i.e.* more sub-bandgap states have been introduced while maintaining the same CB level, then the current density will be lower for any given overall charge density (more traps). We have therefore plotted the extracted charge density (under short-circuit conditions) *versus* the short-circuit photocurrent density over a period of light soaking times for a range of short-circuit currents modulated by the incident light intensity. Initially we observe an *increase* in the photocurrent density for any given charge density, but after a short period, the relationship between charge density and short circuit current remains approximately invariant, despite a continued increase in short-circuit photocurrent density. This, in combination with the observed shift in capacitance toward lower potentials, suggests that the change in capacitance with light soaking is due to a conduction band shift, and not a broadening of the sub-gap DoS.

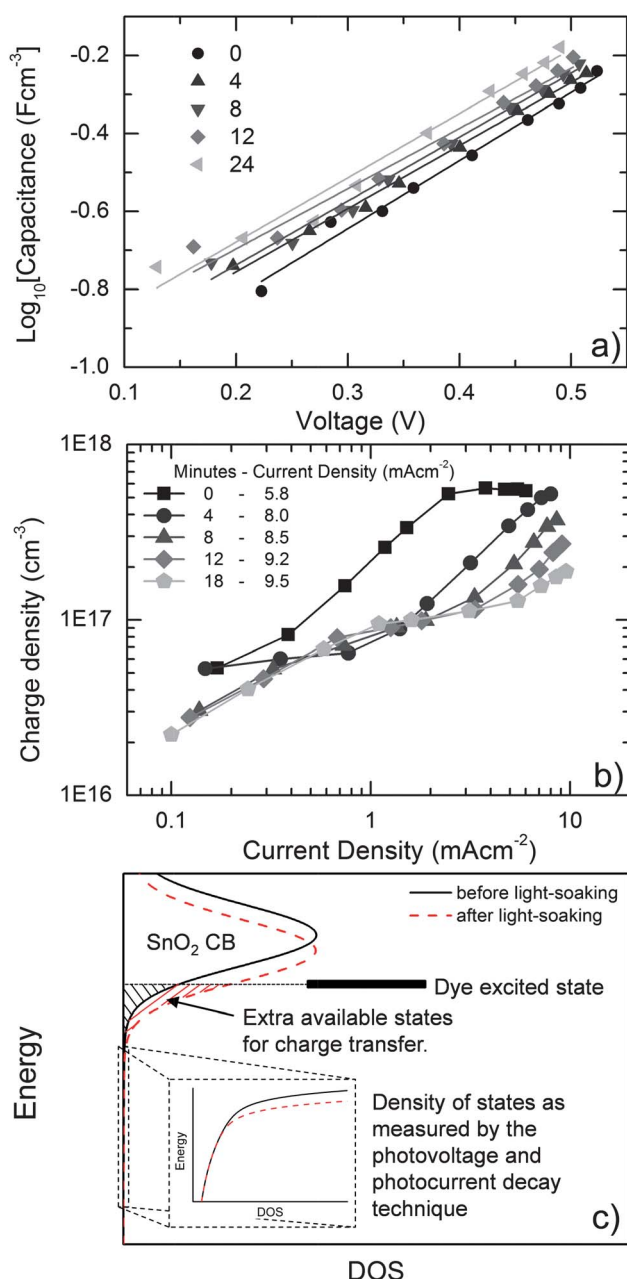


Fig. 4 (a) Change in capacitance *versus* voltage measurement; solid lines represent exponential fits to the experimental data for each light-soaking time, legend indicating the exposure time in minutes. (b) Charge density *vs.* short-circuit current in SnO_2 -MgO/D102 SDSC devices as a function of light-soaking time. Current density shown in legend corresponds to the photocurrent at 100 mW cm^{-2} illumination. The illumination source was red light ($\sim 600 \text{ nm}$), used both for background and perturbation. The measurements were taken every 4 minutes, with the initial measurement shown as black circles and with every consecutive curve shown in a lighter shade of gray than the previous one. (c) Diagram of the expected conduction band shift and its effect on the available states for charge transfer at the level of the dye excited state. The “zoom in” shows the density of states (capacitance) as extracted from the capacitance *versus* voltage measurement. The available states for electron injection pre-light soaking are shaded in black, and for post-light soaking they are cross-shaded in red. We note that the diagram in (c) is purely illustrative.

Table 1 Summary of the evolution of the conduction band shift with light-soaking time

Light-soaking time (min)	CB shift ($\pm 5 \text{ mV}$)
4	20
8	30
12	50
24	70

The relative conduction band shift can be quantified *via* the capacitance measurements by comparing the horizontal displacement of the curves as shown in Fig. 4a. We have observed an approximately 70 mV shift away from vacuum for the devices which have been light-soaked for over 20 minutes. The results are summarized in Table 1.

Although this shift in potential is relatively small, and the increase in capacitance in the sub-gap DoS is only about 20%, in principle, a very small increase in capacitance in the conduction band at the energy at which electron transfer occurs: In Fig. 4c, we show an illustrative Gaussian conduction band with an exponential tail (sub-bandgap states), and shift this by a nominal energy to emulate the light soaking effect. In the inset of this diagram, we zoom into the tail of the DoS in the range which can be normally measured *via* photocurrent and photovoltage decay. With this technique we measure sub-bandgap states which were “full” under illumination at open-circuit and hence the photoinduced electron transfer is unlikely to take place directly into these measured states. The electron transfer is likely to take place directly into the conduction band. In this particular example, we illustrate that the change in the tail of the DoS can be small, whereas at a given energy in the conduction band, the DoS can be increased by over 100%. This arises from the different gradients of the DoS moving from the tail to conduction band states. We note that this is only illustrative, but justifies why a small measured change in capacitance could be highly significant for charge generation. As the density of available states for charge transfer is increased, the electron injection yield from the dye in our devices appears to increase significantly. This correlates well with the increase in photocurrent, observed in Fig. 1. This is also in agreement with previous reports on different preparation methods for mesoporous TiO_2 , where a change in the sub-gap DoS correlates well with increased device photocurrent.^{18,19} Further work is underway to eliminate this effect, thereby obtaining maximum performance immediately upon illumination.

Conclusions

We have observed a steady increase in the short-circuit photocurrent of SnO_2 based solid-state DSCs under illumination, where approximately 20 minutes of AM1.5G light soaking is required to reach maximum efficiency. Through a combined device based and spectroscopic study, we have demonstrated that a systematic enhancement in electron transfer rate leading to enhanced electron transfer efficiency is responsible for the increased photocurrent under visible light illumination. We show that this improved injection is consistent with increasing the

relative density of acceptor states in the SnO₂ at the energy at which electron transfer occurs, which appears to be caused by a conduction band shift of approximately 70 mV, induced by charging of the SnO₂ and a rearrangement of charge species at the dye-sensitized heterojunction.

Experimental details section

Solar cell assembly

Solid-state DSCs (SDSCs) were fabricated on fluorine-doped tin-oxide (FTO) glass (15 Ω □⁻¹ Pilkington) with the desired electrode pattern obtained by etching with ZnO and HCl (2 M). A 100 nm SnO₂ compact layer (CL) was coated on the cleaned and oxygen plasma-treated glass by spray pyrolysis at 450 °C. A fresh batch of butyltin trichloride (95%, Sigma-Aldrich) diluted with ethanol in a 1 : 10 precursor : ethanol ratio was used for each set of devices. During the deposition of the compact layer, the electrodes were masked so that the SnO₂ CL only covered the FTO and not the etched glass.

The SnO₂ paste¹ was then doctor-bladed on the FTO sheets and slowly sintered in air at 500 °C, resulting in 1.8 micron thick SnO₂ films. Some of these films were coated with a subnanometer MgO layer by immersing them in 20 mM magnesium acetate in a boiling ethanol bath maintained at 100 °C for 1 minute, and then resintering them at 500 °C for 45 minutes. All samples were cooled down to 70 °C before dye-sensitization with D102 dye for 1 hour. The samples were quickly rinsed in acetonitrile to remove any dye molecules not physically adsorbed on the semiconductor surface.

Spiro-OMeTAD (2,2',7,7'-tetrakis(*N,N*-dimethoxyphenylamine)-9,9'-spirobifluorene) dissolved in chlorobenzene at 180 mg ml⁻¹ concentration was allowed to wet the dye-sensitized films for 40 s before spin-coating at 2000 rpm for 25 s in air. For every mg of spiro in solution, 0.205 μl of 0.6 M bis(trifluoromethyl-sulfonyl)amine lithium salt (Li-TFSI) solution in acetonitrile and 0.096 μl of *tert*-butylpyridine (*t*BP) were added to the hole transporter solution. The films were allowed to dry in an air atmosphere overnight. Finally, 150 nm thick silver electrodes were evaporated over the HTM layer under high vacuum (10⁻⁶ mbar) to complete the devices.

Samples for OPTP spectroscopy measurements

Samples were prepared by spin-coating SnO₂ paste on z-cut quartz wafers and slowly sintering them at 500 °C, yielding about 1 micron thick transparent mesoporous films. Some of the SnO₂ films were given a conformal MgO coating by dipping them in magnesium acetate in a boiling ethanol bath, as described above. When they cooled down to 70 °C, they were immersed in 0.3 mM Z907 dye solution in acetonitrile-*tert*-butanol (1 : 1 vol%) for about 14 hours at room temperature. As before, the samples were given a quick rinse in acetonitrile, dried for a minute in air, and then stored in the dark in nitrogen atmosphere when not being measured in the OPTP set-up.

Current–voltage measurements

Simulated AM1.5 sunlight at 100 mW cm⁻² irradiance was generated using a class AAB ABET technologies Sun2000 solar simulator calibrated using an NREL calibrated silicon reference

cell with a KG5 filter to minimize spectral mismatch, calculated to be less than 1%.³⁸ *JV* curves were measured with a Keithley 2400 sourcemeter. The solar cells were masked with a metal aperture to define the active area and to minimize any edge effects.

Transient photocurrent and photovoltage measurements

Measurements were carried out using the set-up described in detail elsewhere.^{6,31,39–41} The sample under measurement was biased with white light equivalent to 100 mW cm⁻² solar illumination and perturbed with a red light pulsed diode. The perturbation was kept small enough to ensure that the voltage decay dynamics were approximately monoexponential. Photovoltage transients under short-circuit conditions are measured by holding the current generated by the white light bias fixed at *J*_{SC}. Since no extra current is allowed to flow as a result of the perturbation, the decay of the measured perturbation signal is a direct measure of the rate of charge recombination taking place within the device (*k*_{rec}). On the other hand, photocurrent transients at short-circuit are measured by holding the bias at 0 V, which allows charge transport to occur simultaneously with recombination. The decay rate, therefore, is a combination of *k*_{rec} and the transport rate, *k*_{trans}, as *k*_{signal} = *k*_{trans} + *k*_{rec}. All decay curves were fitted with monoexponentials to estimate the decay rates.

In order to calculate the chemical capacitance (*C*) of the device, the total charge injected from the light pulse (ΔQ) is estimated by integrating the area under the measured current decay curve under short-circuit conditions. The voltage perturbation (ΔV) is extracted from the peak of the voltage perturbation under open-circuit conditions under the same bias light intensity. The capacitance is then calculated as $C = \Delta Q / \Delta V$.

Charge extraction measurements were performed by exposing the device to a constant white background light under short circuit conditions while the photocurrent response is measured with an oscilloscope. Once the device response is stabilized, the white background light is completely switched off and the subsequent photocurrent decay is measured. The charge density is then extracted by integrating the area under the curve for a known active area volume.

Optical pump terahertz probe (OPTP) spectroscopy

800 nm wavelength pulses of about 40 fs duration originating from a 1kHz-repetition-rate Spectra-Physics Spitfire amplifier were used to generate 550 nm pulses in an optical parametric amplifier for photoexciting the dye-sensitized SnO₂ films. The excited sample was then probed after time τ with picosecond duration terahertz (THz) pulses generated using optical rectification by a ZnTe crystal with the Spitfire 800 nm pulses.⁴² Part of the THz pulses interacts with and is absorbed by any mobile charge carriers present in the photoexcited sample. The change in the amplitude and phase of the THz transmitted signal is measured using a double lock-in technique and gives a direct measure of the sample photoconductivity.

All THz pump-probe experiments in this study were performed at room temperature and under vacuum (<10³ mbar pressure). The incident pump fluence was kept low in order to avoid charge–charge interactions, typically at about 10¹³ to 10¹⁴

photons cm^{-2} per pulse.⁴² Also, extremely low energy THz probe pulses are used so that the system is not perturbed by the measurement methodology. Sample integrity was checked before and after the experiments by measuring the steady-state absorption spectrum to verify negligible sample degradation.

Acknowledgements

This work was partly funded by the Engineering and Physical Sciences Research Council (UK) and by the European Community's Seventh Framework Programme (FP7/2007-2013) under grant agreement no. 246124 of the SANS project. PT was in part supported by the Oxford John Fell Fund. We thank Pascal Comte and Michael Grätzel at the École Polytechnique Fédérale de Lausanne for providing the SnO_2 nanoparticle paste. We also thank Monica Lira-Cantu from the Nanoscience and Nanotechnology Research Centre, Barcelona for valuable discussions concerning the light soaking effect.

References

- H. J. Snaith and C. Ducati, *Nano Lett.*, 2010, **10**, 1259–1265.
- A. Kay and M. Grätzel, *Chem. Mater.*, 2002, **14**, 2930–2935.
- K. Tennakone, J. Bandara, P. K. M. Bandaranayake, G. R. A. Kumara and A. Konno, *Jpn. J. Appl. Phys., Part 2*, 2001, **40**, L732.
- Z. M. Jarzelski and J. P. Marton, *J. Electrochem. Soc.*, 1976, **129**, C299.
- E. Yagi, R. R. Hasiguti and M. Aono, *Phys. Rev. B: Condens. Matter Mater. Phys.*, 1996, **54**, 7945–7956.
- P. Tiwana, P. Docampo, M. B. Johnston, H. J. Snaith and L. M. Herz, *ACS Nano*, 2011, **5**, 5158–5166.
- M. K. I. Senevirathna, P. K. D. D. P. Pitigala, E. V. A. Premalal, K. Tennakone, G. R. A. Kumara and A. Konno, *Sol. Energy Mater. Sol. Cells*, 2007, **91**, 544–547.
- A. N. M. Green, E. Palomares, S. A. Haque, J. M. Kroon and J. R. Durrant, *J. Phys. Chem. B*, 2005, **109**, 12525.
- K. Tennakone, P. V. V. Jayaweera and P. K. M. Bandaranayake, *J. Photochem. Photobiol., A*, 2003, **158**, 125–130.
- P. Docampo, N. Sakai, P. Tiwana, H. Miura, L. M. Herz, T. Murakami and H. J. Snaith, *J. Phys. Chem. C*, submitted.
- P. Docampo and H. J. Snaith, *Nanotechnology*, 2011, **22**, 225403.
- B. A. Gregg, S.-G. Chen and S. Ferrere, *J. Phys. Chem. B*, 2003, **107**, 3019–3029.
- S. Ferrere and B. A. Gregg, *J. Phys. Chem. B*, 2001, **105**, 7602–7605.
- A. Hagfeldt, U. Bjorksten and M. Grätzel, *J. Phys. Chem.*, 1996, **100**, 8045–8048.
- B. O'Regan and D. T. Schwartz, *Chem. Mater.*, 1998, **10**, 1501–1509.
- S.-J. Moon, J.-H. Yum, R. Humphry-Baker, K. M. Karlsson, D. P. Hagberg, T. Marinado, A. Hagfeldt, L. Sun, M. Grätzel and M. K. Nazeeruddin, *J. Phys. Chem. C*, 2009, **113**, 16816–16820.
- T. Horiuchi, H. Miura, K. Sumioka and S. Uchida, *J. Am. Chem. Soc.*, 2004, **126**, 12218–12219.
- A. Listorti, C. Creager, P. Sommeling, J. Kroon, E. Palomares, A. Fornelli, B. Breen, P. R. F. Barnes, J. R. Durrant, C. Law and B. O'Regan, *Energy Environ. Sci.*, 2011, **4**, 3494–3501.
- Q. Wang, Z. Zhang, S. M. Zakeeruddin and M. Grätzel, *J. Phys. Chem. C*, 2008, **112**, 7084–7092.
- P. R. F. Barnes, L. Liu, X. Li, A. Y. Anderson, H. Kisserwan, T. H. Ghaddar, J. R. Durrant and B. C. O'Regan, *Nano Lett.*, 2009, **9**, 3532–3538.
- P. R. F. Barnes and B. C. O'Regan, *J. Phys. Chem. C*, 2010, **114**, 19134–19140.
- J. R. Jennings, Y. Liu, F. Safari-Alamuti and Q. Wang, *J. Phys. Chem. C*, 2011, **116**, 1556–1562.
- H. K. Dunn, P.-O. Westin, D. R. Staff, L. M. Peter, A. B. Walker, G. Boschloo and A. Hagfeldt, *J. Phys. Chem. C*, 2011, **115**, 13932–13937.
- J. Navas, E. Guillén, R. Alcántara, C. Fernández-Lorenzo, J. Martín-Calleja, G. Oskam, J. Idígoras, T. Berger and J. A. Anta, *J. Phys. Chem. Lett.*, 2011, **2**, 1045–1050.
- J. P. Gonzalez-Vazquez, J. A. Anta and J. Bisquert, *J. Phys. Chem. C*, 2010, **114**, 8552–8558.
- J. Bisquert and I. Mora-Seró, *J. Phys. Chem. Lett.*, 2009, **1**, 450–456.
- J. Bisquert, F. Fabregat-Santiago, I. Mora-Seró, G. Garcia-Belmonte and S. Giménez, *J. Phys. Chem. C*, 2009, **113**, 17278–17290.
- J. Villanueva-Cab, H. Wang, G. Oskam and L. M. Peter, *J. Phys. Chem. Lett.*, 2010, **1**, 748–751.
- H. K. Dunn and L. M. Peter, *J. Phys. Chem. C*, 2009, **113**, 4726–4731.
- P. Wang, B. Wenger, R. Humphry-Baker, J.-E. Moser, J. Teuscher, W. Kantlehner, J. Mezger, E. V. Stoyanov, S. M. Zakeeruddin and M. Grätzel, *J. Am. Chem. Soc.*, 2005, **127**, 6850–6856.
- P. Docampo, S. Guldin, M. Stefik, P. Tiwana, M. C. Orillall, S. Huttner, H. Sai, U. Wiesner, U. Steiner and H. J. Snaith, *Adv. Funct. Mater.*, 2010, **20**, 1787–1796.
- A. Abrusci, R. S. Santosh Kumar, M. Al-Hashimi, M. Heeney, A. Petrozza and H. J. Snaith, *Adv. Funct. Mater.*, 2011, **21**, 2571–2579.
- J. J. H. Pijpers, R. Ulbricht, S. Derossi, J. N. H. Reek and M. Bonn, *J. Phys. Chem. C*, 2011, **115**, 2578–2584.
- S. E. Koops, B. C. O'Regan, P. R. F. Barnes and J. R. Durrant, *J. Am. Chem. Soc.*, 2009, **131**, 4808–4818.
- P. M. Kumar, S. Badrinarayanan and M. Sastry, *Thin Solid Films*, 2000, **358**, 122–130.
- B. J. Morgan and G. W. Watson, *Surf. Sci.*, 2007, **601**, 5034–5041.
- K. Miettunen, P. R. F. Barnes, X. Li, C. Law and B. C. O'Regan, *J. Electroanal. Chem.*, 2012, **677–680**, 41–49.
- H. J. Snaith, *Energy Environ. Sci.*, 2012, **5**, 6513–6520.
- B. C. O'Regan and F. Lenzmann, *J. Phys. Chem. B*, 2004, **108**, 4342–4350.
- J. Bisquert, A. Zaban, M. Greenshtein and I. Mora-Seró, *J. Am. Chem. Soc.*, 2004, **126**, 13550–13559.
- H. J. Snaith, R. Humphry-Baker, P. Chen, I. Cesar, S. M. Zakeeruddin and M. Grätzel, *Nanotechnology*, 2008, **19**, 424003.
- P. Tiwana, P. Parkinson, M. B. Johnston, H. J. Snaith and L. M. Herz, *J. Phys. Chem. C*, 2010, **114**, 1365–1371.